Effect of Correlated Precision Errors on Uncertainty of a Subsonic Venturi Calibration

S. T. Hudson, W. J. Bordelon Jr., H. W. Coleman

Reprinted from

AIAA Journal

Volume 34, Number 9, Pages 1862–1867

AIAA

A publication of the
American Institute of Aeronautics and Astronautics, Inc.
1801 Alexander Bell Drive, Suite 500
Reston, VA 22091

AIAA JOURNAL
Vol. 34, No. 9, September 1996

Effect of Correlated Precision Errors on Uncertainty of a Subsonic Venturi Calibration

S. T. Hudson* and W. J. Bordelon Jr.†
NASA Marshall Space Flight Center, Huntsville, Alabama 35812
and
H. W. Coleman‡
University of Alabama in Huntsville, Huntsville, Alabama 35899

An uncertainty analysis performed in conjunction with the calibration of a subsonic venturi for use in a turbine test facility produced some unanticipated results that may have a significant impact in a variety of test situations. Precision uncertainty estimates using the preferred propagation techniques in the applicable American National Standards Institute/American Society of Mechanical Engineers standards were an order of magnitude larger than precision uncertainty estimates calculated directly from a sample of results (discharge coefficient) obtained at the same experimental set point. The differences were attributable to the effect of correlated precision errors, which previously have been considered negligible. An analysis explaining this phenomenon is presented. The article is not meant to document the venturi calibration, but rather to give a real example of results where correlated precision terms are important. The significance of the correlated precision terms could apply to many test situations.

Nomenclature

B	= bias limit estimate
C_d	= discharge coefficient
d	= diameter
J	= number of measurement variables
M	= number of tests (measurement sets)
Mn	= Mach number
N	= number of readings
P	= precision limit estimate
p	= pressure
Re	= Reynolds number
r	= result
S	= sample standard deviation
T	= temperature
U	= uncertainty estimate
$\dot{W}$	= mass flow rate
X	= measurement reading
β	= bias component of error
δ	= total error
ϵ	= precision component of error
θ	= sensitivity coefficient
μ	= population mean
ρ	= correlation coefficient
σ	= population standard deviation

Subscripts

0	= total
1	= venturi inlet
2	= venturi throat

Presented as Paper 95-0797 at the AIAA 33rd Aerospace Sciences Meeting, Reno, NV, Jan. 9–12, 1995; received March 15, 1995; revision received March 18, 1996; accepted for publication April 18, 1996.

*Aerospace Engineer, Structures and Dynamics Laboratory. Member AIAA.
†Aerospace Engineer, Structures and Dynamics Laboratory.
‡Eminent Scholar in Propulsion and Professor, Propulsion Research Center, Mechanical and Aerospace Engineering Department. Associate Fellow AIAA.

Introduction

PRECISION uncertainty estimates using the preferred propagation techniques in the applicable American National Standards Institute/American Society of Mechanical Engineers (ASME) standards have traditionally assumed that the correlated precision terms are negligible. This assumption has been made because precision errors are considered to be random. However, the randomness assumption means that there is no correlation among sequential measurements of a single variable. But the real question concerns the correlation of precision errors among simultaneous measurements of different variables. This article presents results from a subsonic venturi calibration as a real example of a case where the correlated precision terms are significant in the uncertainty analysis.

Mass flow venturis are used in a variety of test situations to determine the mass flow rate of gases or liquids. To accurately determine the mass flow rate using a venturi, the discharge coefficient must be known. The discharge coefficient is defined as the ratio of the actual mass flow passing through the venturi to the ideal one-dimensional inviscid mass flow rate. Critical flow venturis are often used because C_d is well known for standard designs such as the Smith–Matz[1] and the ASME[1,2] nozzles. However, a critical flow venturi is not always the most desirable option.[2] When subsonic flowmeters must be used, determination of the discharge coefficient is crucial to meter accuracy.

A subsonic Herschel-type venturi is used in the Turbine Test Equipment (TTE) at the Marshall Space Flight Center (MSFC).[3] The subsonic venturi was chosen over a critical flow venturi to minimize flow noise. The TTE is used to test liquid rocket engine turbines in air at scaled conditions. A technology demonstrator gas generator oxidizer turbine currently is being tested in the TTE.[4] The test data from this technology turbine are to be used for code validation as well as performance evaluation; therefore, absolute accuracy is very important. The mass-flow-rate measurement is used to calculate the turbine efficiency and the turbine flow parameter. The goal of the technology turbine testing is to determine these two performance parameters within ±1%. This means that an accuracy of ±0.5% is needed for the mass flow measurement. The accuracy of the mass flow measurement in the TTE depends on the accuracy of the venturi inlet pressure, throat pressure, and inlet temperature measured during the test; the venturi inlet and throat diameter measured during inspection; and the venturi discharge coefficient determined during calibration. To meet the ±0.5% goal for the TTE mass flow measurement, the discharge coefficient from calibration needs to be determined within approximately ±0.25%.

The TTE venturi had been calibrated, but the stricter requirements for the technology turbine testing prompted a review of the original calibration. This review revealed several concerns. First, the technology turbine would be operating outside the calibration range for the majority of the test matrix. Also, the uncertainty of the standard nozzle used to determine the calibration mass flow rate was ±0.5%. The discharge coefficient uncertainty would thus have been greater than the required ±0.25%.

On the basis of the above findings, it was decided that a new calibration of the TTE venturi was needed. The question was whether or not the venturi could be calibrated to the required ±0.25%. A nine-point test matrix consisting of three venturi throat Mach numbers (0.2, 0.5, and 0.7) and three venturi throat Reynolds numbers (10^6, 3×10^6, and 6×10^6) was decided upon. FluiDyne Aerotest Group of Aero Systems Engineering, Inc. (ASE), was asked to evaluate the uncertainty in C_d that they could obtain in their test facility for this test matrix. ASE estimated a bias error and a precision error for each measurement at each test point. These estimates were then propagated through the data reduction equation for C_d to estimate an uncertainty in the discharge coefficient. On the basis of these estimates, it appeared that the calibration goal of ±0.25% could be achieved at Mach numbers of 0.5 and 0.7 with very careful calibration. However, the low Mach number (0.2) points seemed to be a problem. Large precision errors were predicted at these points because of the low pressure differential between the venturi inlet and throat at these conditions. On the basis of past experience, however, ASE felt that they could achieve better precision with their test system than that predicted. It was decided to proceed with the calibration and to determine the precision limit in the discharge coefficient directly from the test data. Precision limits determined from the test data then would be combined with the bias estimates to determine an overall uncertainty for each test point. These uncertainties would be compared with the pretest predictions and calibration requirement.

When the test data were obtained, two methods of estimating the precision limits in the calibration data were used: 1) calculating the standard deviations for the pressure and temperature measurements and propagating these through the data reduction equation while assuming uncorrelated precision errors and 2) calculating the standard deviations directly from multiple C_d results. The actual test data were used in both cases so that a direct comparison could be made. Method 2 gave precision limits that were an order of magnitude less than those calculated using method 1. The calibration approach, calibration results, and an uncertainty analysis explaining the differences between the two methods of determining the precision limits are discussed.

Calibration Approach

The venturi calibration runs were conducted in air in the Channel 7 test facility at ASE Medicine Lake Aerodynamic Laboratory. The calibration test runs were conducted between Jan. 21 and Feb. 1, 1994. This section describes the experimental setup, measurements, and test procedure as well as details of the test venturi itself. More detailed information is presented in the calibration report.[5]

The venturi used in the MSFC TTE is a Herschel type as defined by Bean.[6] The nominal inlet diameter is 7.980 in., and the nominal throat diameter is 3.396 in. This venturi was sized to operate at subsonic conditions to minimize flow noise or pressure fluctuations caused by a normal shock. The venturi is made of stainless steel and has two instrumentation planes. The venturi inlet plane contains two gas temperature probes and four static pressure taps. The venturi throat contains four static pressure measurements. The overall length of the venturi is 59 in.

The facility used for the venturi calibration was Channel 7 at ASE modified as shown in Fig. 1. The facility consists of a 500-psi air storage source, heater, inlet control valve, ASME metering nozzle, settling chamber, test venturi, and backpressure control valve. The air supply, heater, control valve, metering nozzle, and settling chamber are part of the existing facility setup. An adapter was fabricated to attach the venturi to the settling chamber discharge. Downstream of the venturi, a 16–6-in. reducer was made from standard pipe reducers to install the 6-in. backpressure control valve. The flow was exhausted to atmospheric conditions downstream of the backpressure control valve. Two ASME long-radius metering nozzles were used as the calibration standards to cover the range of calibration conditions. The ASME nozzle nominal throat diameters were 1.47 and 1.75 in. Both nozzles were operated at choked conditions for all test runs.

Pressure and gas temperature measurements were recorded for both the metering nozzle (calibration standard) and the test venturi. The inlet total pressure, two inlet gas temperatures, and a static pressure just downstream of the throat were measured on the metering nozzle. Measurements taken on the test venturi included four inlet static pressures, four throat static pressures, and two inlet gas temperatures. Atmospheric pressure also was measured for each run.

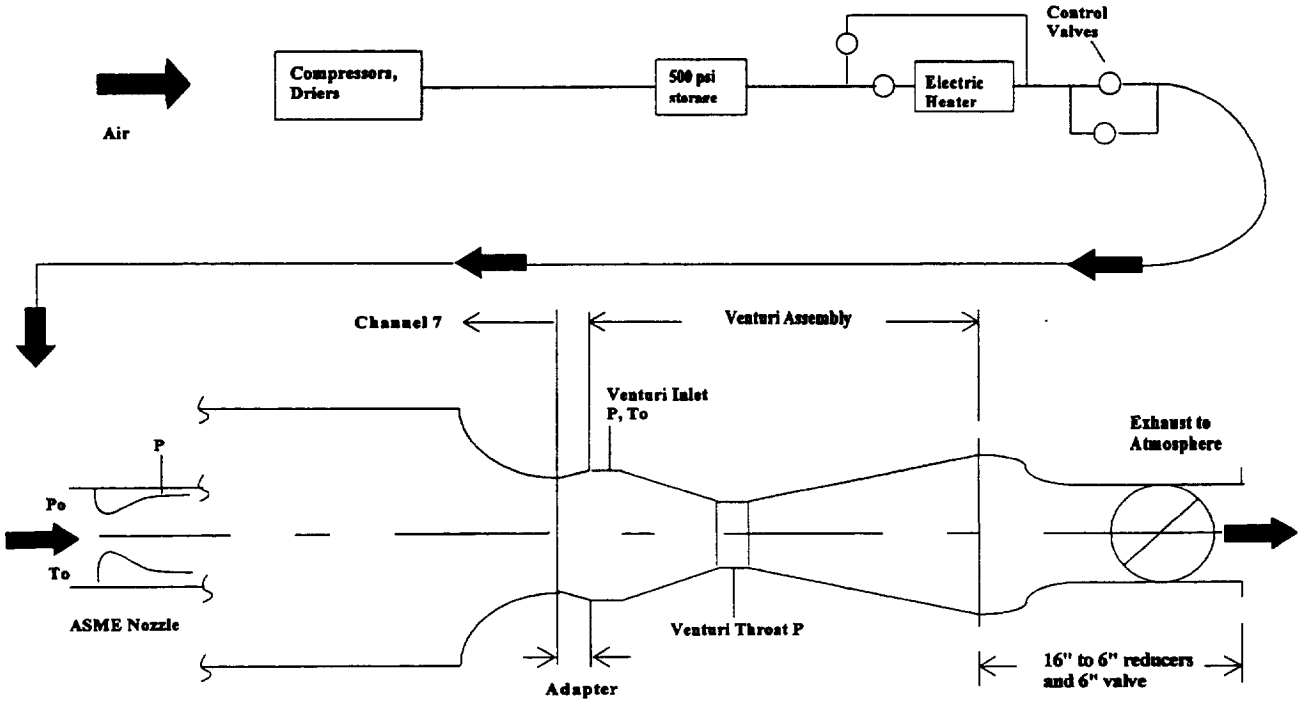

Fig. 1 Venturi calibration schematic (not to scale).

The pressure measurements were made with a Pressure Systems, Inc., pressure scanning system. The metering nozzle gas temperatures were measured with shielded type J thermocouples, and the venturi gas temperatures were measured with type K thermocouples. The voltage outputs from the thermocouples were measured using an electronic digital data acquisition system.

The venturi was calibrated over the range of throat Mach numbers and throat Reynolds numbers by setting the metering nozzle upstream pressure (mass flow for choke condition) with the upstream control valve and the test venturi backpressure with the backpressure control valve. With the metering nozzle choked, the test mass flow and venturi Reynolds number were fixed for a constant metering nozzle inlet total pressure and temperature. The venturi backpressure then was adjusted to set the venturi Mach number. All test runs were conducted with the air at room temperature. Once the test conditions were established, the pressure and temperature measurements were scanned 10 times with about 6 s between each scan.

Calibration Results

The venturi was calibrated over a nine-point test matrix. The nominal throat Mach numbers for this matrix were 0.2, 0.5, and 0.7. The nominal throat Reynolds numbers for this matrix were 10^6, 3×10^6, and 6×10^6. Ten data scans were taken at each set point. The venturi pressures and temperatures were recorded and used to calculate Mn, Re, and C_d for each scan. The equations for these calculations are closed form and are given in the Appendix.[6,7] The 10 scans then were averaged to obtain mean values of Mn, Re, and C_d. Three runs were made (10 scans each, except run 808, which had 9 scans) for the worst-case data point ($Mn = 0.2$, $Re = 10^6$). This was the point where the uncertainty was expected to be the highest. These repeat runs were made to provide more data for understanding the precision behavior associated with this point. The average values of Mn, Re, and C_d for each run are given in Table 1. (Note: At $Mn = 0.7$, Re had to be increased to 1.5×10^6 to achieve the test point.)

Uncertainty Analysis Overview

The word accuracy is generally used to indicate the relative closeness of agreement between an experimentally determined value of a quantity and its true value. Error (δ) is the difference between the experimentally determined value and the truth; thus as error decreases, accuracy is said to increase. Only in rare instances is the true value of a quantity known. Thus, it is necessary to make an estimate of an error, and that estimate is called an uncertainty, U. Uncertainty estimates are made at some confidence level. A 95% confidence estimate, for example, means that the true value of the quantity is expected to be within the $\pm U$ interval about the experimentally determined value 95 times out of 100.

Total error δ can be considered to be composed of two components: a precision (random) component ϵ, and a bias (systematic) component β. An error is classified as precision if it contributes to the scatter of the data; otherwise, it is a bias error. As an estimator of β, a systematic uncertainty or bias limit B is defined. A 95% confidence estimate is interpreted as the experimenter being 95% confident that the true value of the bias error, if known, would fall within $\pm B$. As an estimator of the magnitude of the precision errors, a precision uncertainty or precision limit P is defined. A 95% confidence estimate of P is interpreted to mean that the $\pm P$ interval about a single reading of X_i should cover the (biased) parent population mean μ 95 times out of 100.

Table 1 Calibration results

Run no.	Mn	$Re \times 10^{-6}$	C_d
1.01–1.10	0.197	0.975	0.9899
1.11–1.20	0.192	0.966	0.9917
808.01–808.10	0.201	1.084	0.9866
4.11–4.20	0.199	2.932	0.9894
7.01–7.10	0.199	5.953	0.9933
2.06–2.15	0.502	0.977	0.9885
5.01–5.10	0.495	2.971	0.9914
8.01–8.10	0.493	5.834	0.9927
3.11–3.20	0.698	1.450	0.9907
6.11–6.20	6.695	2.951	0.9914
9.01–9.10	0.683	5.894	0.9938

In nearly all experiments, the measured values of different variables are combined using a data reduction equation (DRE) to form some desired result. A general representation of a DRE is

$$r = r(X_1, X_2, \ldots, X_J) \tag{1}$$

where r is the experimental result determined from J measured variables X_i. Each of the measured variables contains bias errors and precision errors. These errors in the measured values then propagate through the data reduction equation, thereby generating the bias and precision errors in the experimental result r.

If the large sample assumption is made,[8] then the 95% confidence expression for U_r becomes

$$U_r^2 = B_r^2 + P_r^2 \tag{2}$$

where we define the bias limit (systematic uncertainty) of the result as

$$B_r^2 = \sum_{i=1}^{J} \theta_i^2 B_i^2 + 2 \sum_{i=1}^{J-1} \sum_{k=i+1}^{J} \theta_i \theta_k \rho_{\text{bik}} B_i B_k \tag{3}$$

and the precision limit (precision uncertainty) of the result as

$$P_r^2 = \sum_{i=1}^{J} \theta_i^2 P_i^2 + 2 \sum_{i=1}^{J-1} \sum_{k=i+1}^{J} \theta_i \theta_k \rho_{\text{sik}} P_i P_k \tag{4}$$

where ρ_{bik} is the correlation coefficient appropriate for the bias errors in X_i and X_k, ρ_{sik} is the correlation coefficient appropriate for the precision errors in X_i and X_k, and

$$\theta_i = \frac{\partial r}{\partial X_i} \tag{5}$$

The 95% confidence precision limit for a variable X_i can be estimated as

$$P_i = 2S_i \tag{6}$$

where the sample standard deviation for X_i is

$$S_i = \left\{ \frac{1}{N-1} \sum_{k=1}^{N} [(X_i)_k - \bar{X}]^2 \right\}^{\frac{1}{2}} \tag{7}$$

and the mean value for X_i is defined as

$$\bar{X} = \frac{1}{N} \left[\sum_{k=1}^{N} (X_i)_k \right] \tag{8}$$

Traditionally, the correlation terms in Eq. (4) have been assumed to be negligible. This assumption has been made because precision errors are considered random. However, the randomness assumption means that there is no correlation in sequential measurements of a single variable. But, the real question concerns the correlation of precision errors in simultaneous measurements of different variables. These correlation terms may be significant after all.

Single Test: Single Readings

The precision limits defined in Eq. (6) and used in Eq. (4) are applicable to a single test with single readings—that is, at a given test condition, the result is determined once using Eq. (1), and the X_i are considered single measurements. This is the situation often encountered in large-scale engineering tests in which measurements of the variables are made at a given set point over a period that is small compared to the periods of the factors causing variability in the experiment. A proper precision limit (one indicative of the dispersion of the variable over several cycles of the factors causing its variation) cannot be calculated from readings taken over such a small time interval. For such data, the measurement(s) of a variable X_i should be considered a single reading—whether the value of X_i is the average of 10, 10^3, or 10^6 readings taken during the

short measurement time. In such a test, the value for the precision limit to be associated with a single reading would have to be based on previous information about that measurement obtained over the appropriate time interval.[9] If previous readings of a variable over an appropriate interval are not available, then the experimenter must estimate a value for P_i using the best information available at that time.[8,10]

Multiple Tests: Single Readings

If a test is performed so that M multiple sets of measurements $(X_1, X_2, \ldots, X_J)_k$ at the same test condition are obtained, then M results can be determined using Eq. (1), and the best estimate of the result r would be $\bar{r}$, where

$$\bar{r} = \frac{1}{M}\sum_{k=1}^{M} r_k \tag{9}$$

If the M ($M \geq 10$) sets of measurements were obtained over an appropriate time period, the precision limit that should be associated with this averaged result would be

$$P_{\bar{r}} = 2S_r/\sqrt{M} \tag{10}$$

and for a single result would be

$$P_r = 2S_r \tag{11}$$

where S_r is the standard deviation of the sample of M results

$$S_r = \left[\frac{1}{M-1}\sum_{k=1}^{M}(r_k - \bar{r})^2\right]^{\frac{1}{2}} \tag{12}$$

Single Test: Averaged Readings

Some previous approaches[11-13] considered the general case to be that in which the best estimate of the result is determined using averages of the X_i so that

$$r = r(\bar{X}_1, \bar{X}_2, \ldots, \bar{X}_J) \tag{13}$$

and specified that (for large samples) the precision limits be taken as $P_i/(N_i)^{1/2}$ in Eq. (4) (with the correlation terms neglected). The $(\rho_{sik} P_i P_k)$ terms in Eq. (4) take into account the possibility of precision errors in different variables being correlated, and these terms have traditionally been neglected, as mentioned previously. However, precision errors in different variables caused by the same uncontrolled factor(s) are certainly possible, as shown in this article. In such cases, one would need to acquire sufficient data to allow a valid statistical estimate of the correlation coefficients to be made in Eq. (4). Note, however, that the approach using Eqs. (10–12) implicitly includes the correlated error effect—a substantial advantage over the approach of Eq. (13).

Uncertainty Analysis Results

The uncertainty analysis presented here focuses on precision uncertainties. Two methods were used to evaluate the precision limit associated with the experimental result, C_d. First, the precision limit of the result was calculated by propagating the precision of the averaged measured variables through the data reduction equation, as discussed in the paragraph above, while neglecting correlated precision errors (method 1). Equations (4–8) and (13) were used for this approach. Second, the precision limit of the result was calculated directly from the sample standard deviation of C_d for each test point (method 2). Equations (9–12) and (1) were used for this approach. Again, actual test data were used in both cases so that a direct comparison between the two methods could be made. The two methods are discussed, and the results are compared and explained in the following paragraphs.

A Fortran program was written to calculate the precision limit of C_d by the propagation method (method 1). It was assumed that only p_1, p_2, and T_1 contributed to the precision uncertainty:

$$P_{C_d} = P_{C_d}(p_1, p_2, T_1) \tag{14}$$

Table 2 C_d precision results

			P_{C_d}, %	
Mn	$Re \times 10^{-6}$	C_d	Method 1	Method 2
0.197	0.975	0.9899	2.00	0.12
0.192	0.966	0.9917	4.37	0.11
0.201	1.084	0.9866	2.15	0.043
0.199	2.932	0.9894	2.46	0.082
0.199	5.953	0.9933	1.17	0.062
0.502	0.977	0.9885	0.37	0.050
0.495	2.971	0.9914	0.75	0.053
0.493	5.834	0.9927	0.14	0.061
0.698	1.450	0.9907	0.09	0.047
0.695	2.951	0.9914	0.23	0.028
0.683	5.894	0.9938	0.07	0.024

The precision uncertainties associated with the mass flow rate determined by the standard and the test venturi inlet and throat diameters were assumed to be negligible relative to the precision uncertainties of the test venturi measurements of pressure and temperature. The standard deviations S of the three measurements (p_1, p_2, and T_1) were calculated from the 10 data scans for each test run ($N = 10$). The precision limit for each of these mean quantities was then calculated using $P = 2S/(10)^{1/2}$. The values of p_1, p_2, and T_1 were set to the average of the 10 scans for each point. The code used these average values and the precision estimates as inputs for the variables and propagated these values through the DRE to obtain an estimate of the precision limit for C_d. A central-difference numerical scheme was used to approximate the partial derivatives. No correlation of the precision errors in the measured variables was considered.

A summary of the results using the propagation method (method 1) is given in Table 2. These results indicate that the goal of achieving an uncertainty in C_d of ±0.25% cannot be attained. Notice particularly the extremely high precision uncertainties calculated for the low Mach number points.

The precision limit of the discharge coefficient was then determined directly from the C_d results (method 2). C_d was calculated for each data scan. A sample standard deviation S was then computed for each test point using the 10 data scans ($M = 10$). The precision was again calculated using $P = 2S/(10)^{1/2}$. These results also are given in Table 2. The results indicate that the goal of an uncertainty in C_d of ±0.25% can be attained.

The precision limits calculated by method 1 were much higher than those calculated by method 2. The differences were especially large at the low Mach number points. The large uncertainties at the low Mach numbers were attributable to the small difference between the venturi inlet and throat pressures at these conditions. An examination of the influence coefficients obtained from the propagation method revealed that the C_d precision limit was extremely sensitive to the venturi inlet and throat pressure measurements. This sensitivity to the static pressure is discussed elsewhere.[2] The venturi temperature measurement had very little effect on the precision of C_d. The venturi mass flow and, therefore, C_d are functions of the ratio of the inlet to the throat pressure. This means that variations in the inlet pressure and the throat pressure will not affect the precision of $\dot{W}$ or C_d if the ratio remains constant.

The propagation method treated the precision errors in the two venturi pressures as independent. A plot of these two pressures normalized to the critical flowmeter inlet total pressure for a particular run (Fig. 2) shows that the variations of the two pressures are not independent, however. This same trend was seen for all test conditions. The fact that the throat pressure varied with the inlet pressure was a function of the test facility control. The distance between the critical flowmeter and the venturi was small; therefore, pressure variations in the critical flowmeter and in the venturi were in phase. The variations in the pressure measurements were not truly random; they were correlated. This correlation was not accounted for in the propagation analysis. Method 2 automatically accounted for the correlation effect because C_d was calculated for each scan, and these data were used to calculate the precision limit. To account for the correlation effect in the propagation analysis, a correlation coefficient must be estimated. To use this method for pretest

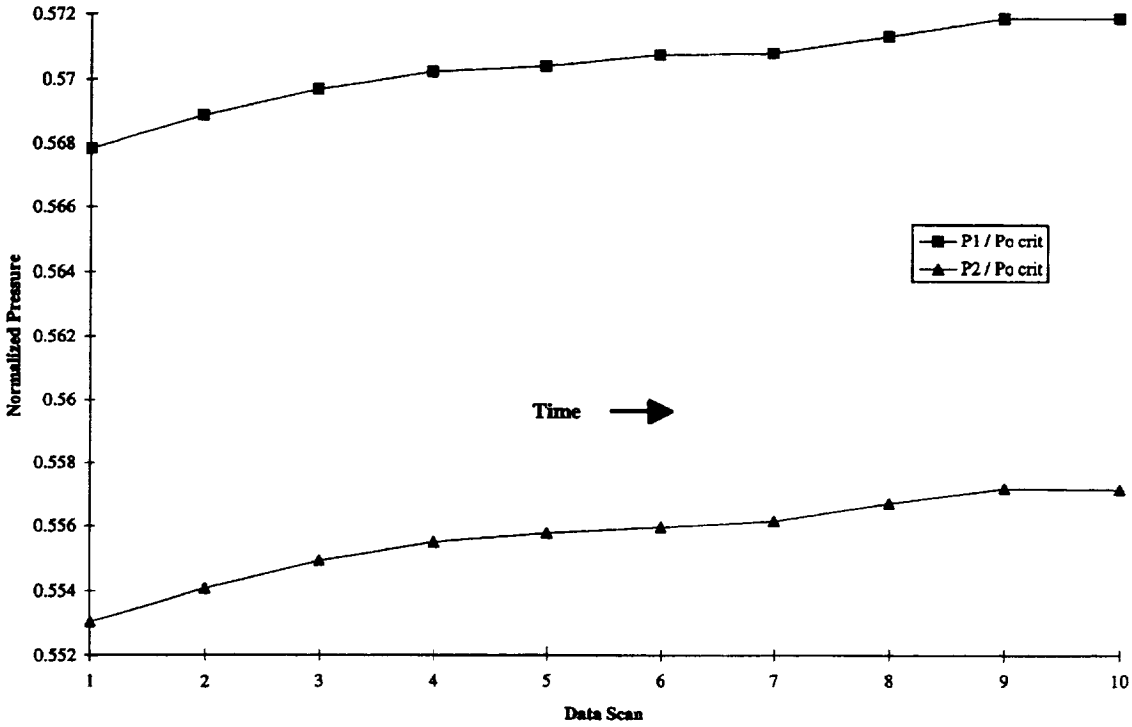

Fig. 2 Normalized venturi inlet and throat pressures.

Table 3 Multiple test results

Run	Mn	$Re \times 10^{-6}$	C_d	P_{C_d}, %
1.01–1.10	0.197	0.975	0.9899	0.12
1.11–1.20	0.192	0.966	0.9917	0.11
808.01–808.10	0.201	1.084	0.9866	0.043
Overall	0.197	1.008	0.9895	0.10

predictions, one must recognize that the precision errors of the two pressures will be correlated and include the correlation terms in the analysis.

Note that the precision limit should be calculated using both methods. Often, the precision limit using method 1 is computed automatically in the data reduction program. When this is done, it is a fairly simple task to add the method 2 calculation of the precision limit to the program. Having the precision limits calculated by both methods would allow one to make a comparison between the two methods. If the precision limits from the two methods are significantly different, then the possibility of having correlated precision effects should be evaluated.

To gain more insight into the precision of the worst-case point of $Mn = 0.2$ and $Re = 10^6$, three runs were made at this test condition. Two of the runs (10 scans each) were made at different times on the same day, and the third run (9 scans) was made almost two weeks later. The data for each run were calculated by method 2, as discussed previously. Combining the three runs gave $M = 29$ for the overall data set. These data are summarized in Table 3. The data show that the run-to-run repeatability is good. Some variation in C_d is expected because of set-point variations. The precision limit of the overall average discharge coefficient is 0.10% when all three runs are considered [$P = 2S/(29)^{1/2}$]. This data set allows one to be more sure of the precision of the worst-case point.

Conclusions

Correlated precision terms can have a significant effect on the precision limit of a result. Precision uncertainty estimates using propagation techniques without considering correlated precision terms were an order of magnitude larger than precision uncertainty estimates calculated directly from a sample of results obtained at the same experimental set point. The potential effect of correlated precision terms makes it better to use multiple results rather than the propagation method to determine a precision limit for a result. The propagation method is useful in the planning phase, but one must recognize the effect of the correlated precision terms and include this in the analysis if it is applicable in a particular test situation. When the precision limit is automatically computed in the data reduction program, it should be computed by both methods so that a comparison can be made. If the precision limits are significantly different, then the possibility of having correlated precision effects should be considered. The correlated precision effect is probably much more prevalent than considered in the past, because it occurs in any system in which multiple variables drift in unison in response to unsteadiness during the testing period.

Acknowledgments

The venturi calibration test by ASE was conducted for MSFC through Dynamic Engineering, Inc. (DEI). J. R. Herdy was the DEI technical monitor for the contract, and W. J. Kauffman Jr. was the NASA employee responsible for the venturi calibration. J. P. Heaman of NASA also provided valuable input. The work by ASE and these individuals to make the calibration a success is greatly appreciated. Also, thank you to C. E. Hudson Jr. for assisting with the raw data tables for the uncertainty analysis.

Appendix: Equations

The equations used to calculate the venturi Mach number, Reynolds number, mass flow rate, and discharge coefficient for this application are included here. The basic equations came from Bean,[6] and they are applied to this specific case elsewhere.[7] (Note that the equations for Mach number and Reynolds number are the same as those used by ASE,[5] but the equation for mass flow is different.) The equations are written for English units; therefore, pressure must be in psia, area in square inches, and temperature in °R. Constants used include $\gamma = 1.4$ and $R = 53.35$ ft-lb$_f$/lb$_m$°R. The symbol ρ is now used for density (ρ was the correlation coefficient in the text of the article). Also, the symbol M (not Mn) is now used for Mach number. The constant 9.9×10^6 in Eq. (A7) is the thermal expansion coefficient.

Venturi diameter ratio and pressure ratio:

$$DR = d_2/d_1; \qquad PR = p_2/p_1 \tag{A1}$$

Throat Mach number:

$$M_2 = \sqrt{5\left[\frac{PR^{-\frac{2}{7}} - 1}{1 - (DR^4)\left(PR^{\frac{10}{7}}\right)}\right]} \tag{A2}$$

Inlet Mach number:

$$M_1 = DR^2 PR^{\frac{6}{7}} M_2 \tag{A3}$$

Inlet static temperature:

$$T_1 = \frac{T_{o_1}}{1 + 0.2M_1^2} \tag{A4}$$

Inlet density:

$$\rho_1 = \frac{144 p_1}{RT_1} \tag{A5}$$

Throat adiabatic wall temperature:

$$T_{2aw} = T_{o_1}\left(\frac{1 + 0.1784M_2^2}{1 + 0.2M_2^2}\right) \tag{A6}$$

Throat diameter corrected because of difference between operating temperature and room temperature:

$$d_{2_T} = d_2\left[1 + 9.9 \times 10^{-6}(T_{aw} - 529.67)\right] \tag{A7}$$

Throat area based on throat diameter in Eq. (A7):

$$A_{2_T} = \pi\left(d_{2_T}/2\right)^2 \tag{A8}$$

Throat Reynolds number per foot per psia:

$$\frac{Re}{dp_{o_2}} = \frac{(181,176,192)M_2\left[T_{o_1} + 198.6\left(1 + 0.2M_2^2\right)\right]}{\left(T_{o_1}\right)^2\left(1 + 0.2M_2^2\right)^{2.5}} \tag{A9}$$

Throat Reynolds number:

$$Re = Re_2 = (Re/dp_{o_2})p_2\left(1 + 0.2M_2^2\right)^{3.5}\left(d_{2_T}/12\right) \tag{A10}$$

Ideal mass flow rate (lb_m/s):

$$\dot{W}_{\text{ideal}} = \dot{W}_2 = 1.250605\left(A_{2_T}\right)\left[\frac{p_1\rho_1 PR^{\frac{10}{7}}\left(1 - PR^{\frac{2}{7}}\right)}{1 - DR^4 PR^{\frac{10}{7}}}\right]^{\frac{1}{2}} \tag{A11}$$

Discharge coefficient:

$$C_d = \frac{\dot{W}_{\text{standard}}}{\dot{W}_{\text{ideal}}} = \frac{\dot{W}_{\text{actual}}}{\dot{W}_{\text{ideal}}} \tag{A12}$$

References

[1]Smith, R. E., and Matz, R. J., "A Theoretical Method of Determining Discharge Coefficients for Venturis Operating at Critical Flow Conditions," *Journal of Basic Engineering*, Dec. 1962, pp. 434–446.

[2]Lahti, D. J., "Theory and Experiments on Subcritical Compressible Gas Flow Metering," Ph.D. Dissertation, Dept. of Aerospace Engineering and Applied Mechanics, Univ. of Cincinnati, OH, Aug. 1990.

[3]Bordelon, W. J., Jr., Kauffman, W. J., Jr., and Heaman, J. P., "The Marshall Space Flight Center Turbine Test Equipment; Description and Performance," American Society of Mechanical Engineers, ASME 93-GT-380, New York, 1993.

[4]Hudson, S. T., Johnson, P. D., and Wooler, A., "Baseline Design of the Oxidizer Technology Turbine Rig," Advanced Earth-to-Orbit Propulsion Technology Conf., Huntsville, AL, May 1994.

[5]Hanson, P. J., and Reeve, R. E., "Airflow Calibration of a Venturi Assembly," FluiDyne, Aerotest Group Rept. 2013, St. Paul, MN, Feb. 1994.

[6]Bean, H. S. (ed)., *Fluid Meters, Their Theory and Application*, 6th ed., American Society of Mechanical Engineers, New York, 1971, pp. 47–80.

[7]Davis, M. W., "Calibration of Two Herschel Venturis for the Turbine Test Equipment," Sverdrup Technology Memo, March 1988.

[8]Anon., "Assessment of Wind Tunnel Data Uncertainty," AGARD-AR-304, 1994.

[9]Steele, W. G., Taylor, R. P., Burrell, R. E., and Coleman, H. W., "Use of Previous Experience to Estimate Precision Uncertainty of Small Sample Experiments," *AIAA Journal*, Vol. 31, No. 10, 1993, pp. 1891–1896.

[10]Coleman, H. W., and Steele, W. G., *Experimentation and Uncertainty Analysis for Engineers*, Wiley, New York, 1989.

[11]American National Standards Institute/American Society of Mechanical Engineers, *Measurement Uncertainty*, PTC 19.1-1985, Pt. 1, American Society of Mechanical Engineers, New York, 1986.

[12]American National Standards Institute/American Society of Mechanical Engineers, *Measurement Uncertainty for Fluid Flow in Closed Conduits*, MFC-2M-1983, American Society of Mechanical Engineers, New York, 1984.

[13]Abernethy, R. B., Benedict, R. P., and Dowdell, R. B., "ASME Measurement Uncertainty," *Journal of Fluids Engineering*, Vol. 107, 1985, pp. 161–164.